Anomalous transport in mesoscopic inhomogeneous two-dimensional electron systems at low temperature

D. Neilson
Dipartimento di Fisica, Università di Camerino, I-62032 Camerino, Italy and NEST CNR-INFM, I-56126 Pisa, Italy

A. R. Hamilton
School of Physics, University of New South Wales, Sydney 2052, Australia

(Received 22 January 2010; published 20 July 2010)

We analyze transport properties of mesoscopic GaAs two-dimensional (2D) electron systems in the insulating regime. It is well known that disorder can cause the insulating system to break up into connected insulating domains and isolated conducting domains. In mesoscopic systems the separation between conducting domains can be very small even when $\rho \gg h/e^2$. In this case, transport at sufficiently low temperatures, $T \lesssim 1$ K, is controlled not by conventional hopping but by short-range tunneling between adjacent conducting domains, and this has a dramatic effect on the low-T transport properties. The resulting T-dependent resistivity $\rho(T)$ is in good agreement with measurements of $\rho(T)$ in 2D electron layers in gated mesoscopic GaAs/AlGaAs structures and, in particular, $\rho(T)$ can even exhibit an anomalous metalliclike drop as $T \to 0$ even for resistivities ρ as high as $\sim 500 h/e^2$.

DOI: 10.1103/PhysRevB.82.035310 PACS number(s): 73.21.−b, 73.20.Jc, 73.40.−c

Transport properties of dilute two-dimensional (2D) electron systems are determined by a subtle combination of the effects of disorder and the repulsion between electrons. Both Anderson[1] and Mott[2] considered the detailed form of the quantum-mechanical wave function for the electrons. Anderson showed that the effects of microscopic disorder acting on this wave function can lead to localization, while Mott, following a suggestion by Peierls[3] showed that the repulsion between electrons can cause a quantum metal-insulator transition from a conducting metallic ground state to an insulating ground state. By contrast, Landauer,[4] Keyes,[5] and others, emphasized the inhomogeneous nature of disordered systems. The classical charging effects associated with such inhomogeneous systems can lead to a percolation transition in the transport.[6]

There is growing experimental evidence for spatial inhomogeneities in 2D systems and the formation at low electron densities of inhomogeneous metallic and insulating domains.[7–9] Studies of the compressibility of 2D systems in GaAs heterostructures show evidence for inhomogeneities in modulation-doped samples,[10] and there is evidence for a percolation driven metal-insulator transition in a dilute 2D GaAs electron and hole systems even in the absence of modulation doping.[11–13] Davydov *et al.*[14] have shown that electron transport near the metal-insulator transition is controlled by saddle-point potential barriers between conducting domains in metal-nitride-oxide-semiconductor silicon transistors. Adam *et al.*[15] have reported evidence of a percolation-driven metal-insulator transition in a graphene nanoribbon caused by random charged impurity centers. A theoretical approach using coexisting metallic and insulating domains have been employed by Shimshoni *et al.*[16] to study transport properties for quantum-Hall insulators and superconductors, and Meir[17] and Neilson *et al.*[18] used a domains model to study transport near the $B=0$ 2D metal-insulator transition.

In 2D modulation-doped GaAs/AlGaAs heterojunctions, the main source of disorder comes from the remote charged dopant ions, which is long ranged. Imaging of the disorder in these systems using a scanning charge probe suggests the dominant disorder length scale is greater than 0.5 μm.[19,20] This is much greater than the typical widths of the undoped spacer layer separating the 2D electron system from the dopants, and indicates that long-range disorder dominates on a macroscopic length scale. The inhomogeneous charge distribution and random potential are illustrated in Figs. 1(a) and 1(b) for a macroscopic 2D sample.

Baenninger *et al.*[21] have suggested that the effects of

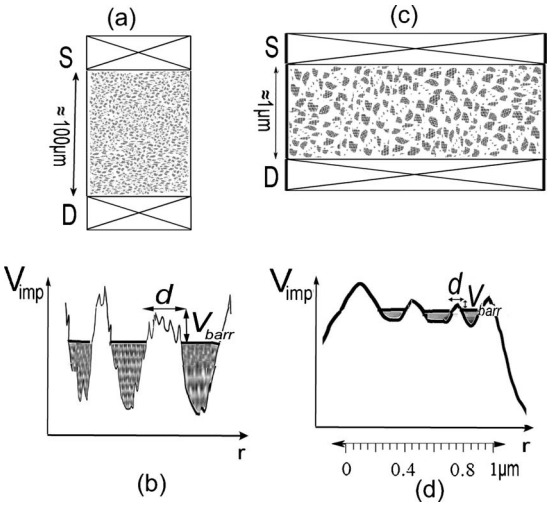

FIG. 1. (a) Schematic of macroscopic sample in the insulating regime with isolated metallic domains (shaded regions) of average size 0.1 μm separated by insulating regions (white). S: source terminal; D: drain terminal. (b) Disorder potential $V_{imp}(\mathbf{r})$ in modulation-doped macroscopic sample with typical barrier height $V_{barr} \sim 2-5$ meV and barrier width $d \gtrsim 10$ nm. (c) Schematic of wide mesoscopic sample. (d) $V_{imp}(\mathbf{r})$ in mesoscopic sample with $V_{barr} \sim 0.5$ meV and $d \lesssim 5$ nm.

long-range disorder can be eliminated and transport studied in the presence of the weaker residual short-range disorder by working in short mesoscopic systems with lengths less than the long-range disorder length scale. This geometry is illustrated in Figs. 1(c) and 1(d). Reference 21 observed significant differences in the temperature dependence of the resistivity $\rho(T)$ between macroscopic samples on the one hand and mesoscopic samples with lengths much shorter than the long-range disorder length scale on the other. In the macroscopic samples, familiar exponential growth in $\rho(T)$ was observed with decreasing T. However in the mesoscopic samples, there was a marked and surprising change in the low-T properties. This can clearly be seen in the experimental data points reproduced from Fig. 2 in Ref. 21. In the mesoscopic samples the exponential growth was sustained only down to temperatures ~ 1 K. For $T \lesssim 1$ K, Baenninger *et al.* found that $\rho(T)$ either saturated or that it even turned over and actually decreased as T was lowered. A saturation or metalliclike decrease in $\rho(T)$ is surprising, especially as these effects were seen deep in the insulating region out to resistivities as high as $\rho \sim 500h/e^2$.

In this work we propose that the observed saturation and/or turnover of $\rho(T)$ at low T is evidence for the inhomogeneous nature of even these short high mobility 2D electron systems, along the lines suggested by Landauer and Keyes.[4,5] In the large-ρ transport regime ($\rho \gg h/e^2$), the electrons are confined to isolated metallic domains surrounded by insulating regions, and are delocalized within the metallic domain with an effective localization length much larger than the Bohr radius. This is very different to the pictures put forward by Anderson and by Mott of transport in homogeneous systems where the electrons are strongly localized to charged impurity sites and transport occurs via variable range hopping.[22] In contrast, in the presence of isolated metallic domains, low-temperature transport deep in the insulating phase is determined by tunneling through a potential barrier separating states of equal energy that lie on the boundaries of neighboring metallic domains. Our proposal that the system is inhomogeneous is consistent with the density dependence of the resistivity measured at low T in the mesoscopic samples of Ref. 21, which show reproducible nonmonotonic fluctuations (Fig. 3) instead of the smooth dependence on gate voltage that would be expected for a uniform system.

In order to determine the transport properties at low temperatures we start by considering the state of an inhomogeneous 2D system at the percolation threshold. The system consists of insulating and metallic domains, and we imagine a crossing of the ground state energies $E_M(\mu_c)=E_I(\mu_c)$ of the metal and insulator, respectively, at a critical value μ_c of the chemical potential μ. The percolation threshold in 2D occurs when the total areas of the two types of domains are equal.[16] At the threshold, there is at least one continuous conducting path across the sample. When we move into the insulating phase there is no longer a continuous conducting path, instead conduction is via a network of tunnel junctions. As the electron density is reduced the metallic domains slowly retreat from each other and are separated by insulating domains (Fig. 1). It is important to recognize that in the mesoscopic systems the average width d of the barriers separating metallic domains can still be small even deep inside the insulator region. This is because at very low temperatures the dominant mechanism is tunneling, and tunneling rates will decrease exponentially with d.

The boundaries $\mathbf{R}_b$ of the metallic domains in the insulating phase follow the equipotential contours $V_{imp}(\mathbf{R}_b)=\mu-\mu_c$, where $V_{imp}(\mathbf{r})$ is the random impurity potential. In the insulating region that separates adjacent metallic domains the $V_{imp}(\mathbf{r})$ forms a saddle point centered on μ_c,

$$V_{imp}(\mathbf{r}) = \mu_c - (1/2)m(\omega_x^2 x^2 - \omega_y^2 y^2). \tag{1}$$

The parameters $m\omega_x^2$ and $m\omega_y^2$ characterize the curvature of the saddle point in the direction of electron transport and in the transverse direction, respectively. Conduction across the sample is via a network of metallic domains (see Fig. 1). The primary contribution to the resistivity comes from tunneling across the potential barrier separating metallic domains. For a 2D array of tunnel junctions, the total resistance is determined by the resistance of the most resistive junction.[17,23]

To calculate the transport properties, we determine $\rho(T)$ from the transmission across this tunnel junction as a function of the barrier width d that separates it from the adjacent metallic domain. The resistivity depends on the transmission probability $\mathcal{T}(T)$ through the junction, $\rho(T)=[1-\mathcal{T}(T)]/\mathcal{T}(T)$, in units of h/e^2. Initially we will assume that the quantum interference effects take place on a length scale small compared with the size of the domains ℓ_V, so there is no coherence between successive tunneling events.

At relatively high T the tunneling is thermally assisted between two states of, in general, different energies located within the adjacent metallic domains. For $\rho \gg 1$, the Fermi energy lies well below the potential at the saddle point so the semiclassical approximation can be applied and the transmission is given by

$$\mathcal{T}_{th}(T) \sim \int_{V_{barr}}^{\infty} \exp(-E/k_BT)dE$$
$$= \mathcal{T}_{d=0} \exp\left(-\frac{V_{barr}}{k_BT}\right), \quad \text{larger } T. \tag{2}$$

The potential barrier height across the junction V_{barr} is related to the curvature of $V_{imp}(r)$ at the junction,

$$V_{barr} = \mu_c - (1/2)m\omega_x^2(d/2)^2. \tag{3}$$

The prefactor $\mathcal{T}_{d=0}$ is the transmission across the junction for $d=0$. We will find in the mesoscopic samples that the tunnel width d is only a few nanometers. This is much less than the Fermi wavelength at these electron densities, so $\mathcal{T}_{d=0}$ is in general less than unity.

At low enough temperature, the transmission will be dominated instead by tunneling between states of the same energy lying on the equipotential contours $\mu=\mu_c$ that form the boundaries of the metallic regions. The transmission is given within the semiclassical approximation by the temperature-independent expression

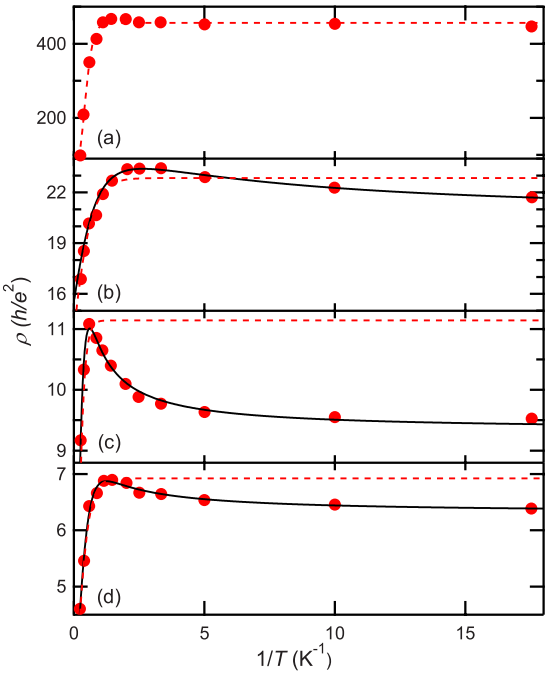

FIG. 2. (Color online) Resistivity $\rho(T)$ as a function of inverse temperature. Experimental data points in red are taken from the same sample in Ref. 21 at different gate biases: (a) Fig. 2a of Ref. 21; (b) Fig. 2(b); (c) Fig. 2(c); and (d) Fig. 2(d). Dashed red lines are calculated using Eq. (6). Solid black lines in panels (b)–(d) are calculated using Eq. (11).

$$\mathcal{T}_{tun} \simeq \mathcal{T}_{d=0} \exp(-S''d^2). \tag{4}$$

S'' is the second derivative of the action across the barrier $S(d)$, given by $S''=(\pi/2\hbar)\sqrt{m(\partial V_{imp}/\partial x)}=(\pi/2\hbar)m\omega_x$, and so Eq. (4) can be written as

$$\mathcal{T}_{tun} = \mathcal{T}_{d=0} \exp[-(\pi/\hbar)\sqrt{2mV_{barr}}d], \quad \text{small } T. \tag{5}$$

Thus with decreasing T, we expect the resistivity to initially increase exponentially [Eq. (2)] but then at low T it should saturate to a constant value [Eq. (5)]. Interpolating between the limiting expressions for the transmission, Eqs. (2) and (5), we write

$$\rho(T) = \left\{ \mathcal{T}_{d=0} \exp\left[-\frac{\pi\sqrt{2mV_{barr}}}{\hbar} d \right] + \mathcal{T}_{d=0} \exp\left[-\frac{V_{barr}}{k_B T} \right] \right\}^{-1} - 1. \tag{6}$$

We used Eq. (6) to fit the measured T-dependent resistivity data from Fig. 2 of Ref.21, which are reproduced as the data points in Fig. 2 of this paper. The dashed lines in Fig. 2 show the fits of Eq. (6) to the experimental points. Table I (a) gives the fitting parameters $\mathcal{T}_{d=0}$, d, and V_{barr}, for the electron densities n from Fig. 2. As expected, $\mathcal{T}_{d=0}$ increases and d decreases with n, although there is no systematic trend for V_{barr}.

We conclude that Eq. (6) reproduces most features of the experimental data well but it does not account for the turndown in the $\rho(T)$ observed in some of the cases for $T \lesssim 1$ K. Even though the turndown in the $\rho(T)$ is not a large effect, at maximum 10% of the total resistance, nevertheless a model of tunneling at a single junction cannot produce a drop in $\rho(T)$.

TABLE I. (a) Fitted values of zero-width transmission $\mathcal{T}_{d=0}$, tunneling distance d, and barrier height V_{barr} for the data in Fig. 2 of Ref. 21. Column A lists panels from our Fig. 2. n is electron density. (b) Fitted values of coherent transmission rate $\mathcal{T}_{coh}$ and ratio ℓ_v/ℓ.

(a) A	n 10^{10} cm^{-2}	$\mathcal{T}_{d=0}$	d (nm)	V_{barr} (meV)
a	0.94	0.03	4.9	0.55
b	1.15	0.03	2.4	0.16
c	1.39	0.15	1.2	0.64
d	1.65	0.15	0.4	0.36

(b) A	$\mathcal{T}_{coh}$	ℓ_v/ℓ
b	0.033	14.2
c	0.20	1.5
d	0.17	4.7

The cause of the drop in resistance could be onset of coherent tunneling. Up to now we have assumed, as in Ref. 17, that the size of the metallic domain is sufficiently large for the electrons to always have time to decohere between tunneling through junction "*i*" into the metallic domain, and then tunneling through junction "*o*" out of the same domain. Denoting the corresponding transmission probabilities by $\mathcal{T}_i$ and $\mathcal{T}_o$, the incoherent transmission rate across the metal domain is

$$\mathcal{T}_{incoh} = \mathcal{T}_i\mathcal{T}_o/(\mathcal{T}_i + \mathcal{T}_o). \tag{7}$$

Without loss of generality we can make i the most resistive junction in the 2D network of junctions, so then $\mathcal{T}_i \le \mathcal{T}_o$, and

$$\mathcal{T}_i/2 \le \mathcal{T}_{incoh} \le \mathcal{T}_i. \tag{8}$$

It is clear that the assumption of incoherent propagation must break down at sufficiently small T since the coherence length ℓ_ϕ, the characteristic scale for coherent propagation, is inversely proportional to temperature. In macroscopic 2D samples in the metallic regime, $\ell_\phi=(\hbar k_F D)/(\pi T)=\hbar^2 k_F^2 \ell/(2\pi m k_B T)=(T_F/T)(\ell/\pi)$, where ℓ is the mean-free path for elastic scattering. Thus at these electron densities for which the Fermi temperature $T_F \sim 5$ K, the coherence length ℓ_ϕ approaches the mean-free path ℓ when $T \sim 1$ K. The ℓ itself will be bounded by the metallic domain length scale ℓ_v. As T decreases below $T=1$ K, ℓ_ϕ will therefore approach ℓ_v, making coherent propagation across the entire metallic domain increasingly likely.[24]

In the $T \to 0$ limit for coherent propagation, the peak value of the transmission for an electron at the resonance energy is

$$\mathcal{T}_{coh,res} = 4\mathcal{T}_i\mathcal{T}_o/(\mathcal{T}_i + \mathcal{T}_o)^2. \tag{9}$$

Since $\mathcal{T}_i \le \mathcal{T}_o$,

$$\mathcal{T}_{coh,res} \geq \mathcal{T}_i/\mathcal{T}_o \geq \mathcal{T}_i \geq \mathcal{T}_{incoh}. \tag{10}$$

We represent the zero-temperature transmission rate from coherent propagation across the metal domain averaged over electron energies with the parameter $\mathcal{T}_{coh}$, where $\mathcal{T}_{coh} \leq \mathcal{T}_{coh,res}$. Adding $\mathcal{T}_{coh}$ into Eq. (6) we write

$$\rho(T) = \left\{ [\mathcal{T}_{d=0}(1 - p_{coh}(T)) + \mathcal{T}_{coh} p_{coh}(T)] \times \exp\left[- \frac{\pi\sqrt{2mV_{barr}}}{\hbar} d \right] + \mathcal{T}_{d=0} \exp\left[- \frac{V_{barr}}{k_B T} \right] \right\}^{-1} - 1, \tag{11}$$

$p_{coh}(T) = \exp[-\ell_v/\ell_\phi] = \exp[(-\ell_v/\ell)(\pi T/T_F)]$ is the probability that an electron traverses the metallic domain without scattering.

We used Eq. (11) to fit again the $\rho(T)$ data in Ref. 21 for the cases for which a turnover in $\rho(T)$ is observed, Figs. 2(b)–2(d). We could satisfactorily fit the additional parameters, the coherent transmission $\mathcal{T}_{coh}$ and the ratio (ℓ_v/ℓ), without changing the parameters from (a) in Table I. The solid lines in panels (b)–(d) in Fig. 2 show the resulting good fits to the experimental points. Values of $\mathcal{T}_{coh}$ and (ℓ_v/ℓ) are given in (b) in Table I.

While our analysis gives barrier heights and widths for the junctions between metallic domains, it gives no information about the size of the domains. Values of the length scale of the disorder variation, $\ell_{disorder} \sim 0.5-1.5$ μm, have been measured in macroscopic samples by Finkelstein *et al.*[19] and by Chakraborty *et al.*[20] The variations in $\Delta V_{disorder} \sim 2-5$ meV reported in Refs. 19 and 20 are much larger than the values of $V_{barr} \lesssim 0.5$ meV in Table I. This is consistent with the suggestion in Ref. 21 that in mesoscopic samples with lengths less than the length scale of the disorder variation in the long-range disorder, it is the much weaker potential fluctuations of the residual disorder that dominate the transport. Furthermore, if we fit the prefactor for the exponential growth in $\rho(T)$ for the macroscopic samples of Ref. 21 we find $\mathcal{T}_{d=0} \sim 1$. This suggests for the macroscopic samples that the width of the saddle-point potential separating the metallic domains is greater than the Fermi wavelength $\lambda_F \sim 250$ nm, and hence much larger than the values for $d \lesssim 5$ nm that we have determined for the mesoscopic samples [see (a) in Table I].

In the mesoscopic samples, the domains cannot be larger than the sample length, ~ 0.5 μm,[21,25] and with metallic domains as small as this, one might expect Coulomb blockade and energy quantization effects to be important. Indeed in 50% of the samples studied in Ref. 21 Coulomb blockade was observed, and these were not considered further in the experiments. There are two reasons why Coulomb blockade and energy quantization effects do not dominate all samples. First, the relatively low potential barriers separating neighboring metallic domains for the mesoscopic samples will tend to smear out these effects. Each metallic domain in the conducting path has at least two tunnel junctions connecting it to adjacent domains. Even for the metallic domain with the most resistive junction i, it is unlikely that the second tunnel junction o is equally resistive, and this will lead to significant broadening of the energy levels in the metallic domain, since the electron can relatively easily escape through junction o. Broadening of the energy levels will reduce resonance effects.

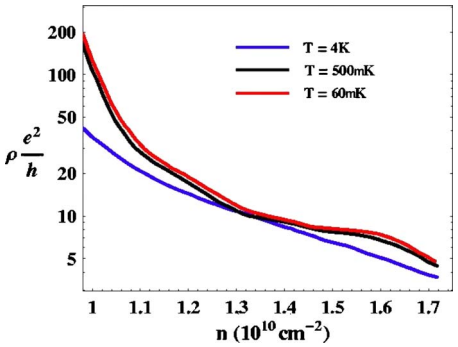

FIG. 3. (Color online) Resistivities taken from Ref. 21 as function of electron density n for fixed temperatures (from bottom) T = 4 K, 500 mK, and 60 mK.

A second reason for the absence of Coulomb-blockade effects is the large width-to-length ratio for these mesoscopic samples. Should one particular percolation path across the sample become completely Coulomb blockaded, the large ratio ensures that there are many other percolation paths to transport the electrons. The large number of paths has the effect of averaging out fluctuations arising from resonance effects. Some modulation of the conductance as a function of gate voltage is still visible in the data (see Fig. 3), which points to residual resonance effects.

There are parallels in this argument with the work of Popović *et al.*,[26] who also used short wide samples with similar width-to-length ratios as here. However while Popović *et al.* were searching for transmission through a single impurity, here we are proposing that the transmission is determined by tunneling between adjacent metallic domains of the most resistive junction. It would be of interest to compare the measurements in Ref. 21 with a new set of transport measurements for long and narrow mesoscopic samples with the inverse width-to-length ratio. A narrow sample would greatly limit the number of possible parallel percolation paths across the sample, making it much more probable that every percolation path would have to pass through at least one small domain in which there was Coulomb blockade at low temperatures.

Our picture leads to other characteristic behaviors in inhomogeneous mesoscopic samples. The Hall voltage should be strongly affected by the inhomogeneities in the sample, which cause a nonuniform current distribution within the sample, and therefore a nonlinear evolution of the Hall voltage with magnetic field. This has recently been observed.[27] With dc bias, if transport is indeed through a network of barriers and metallic domains, one might expect to observe

features also seen in quantum dots and quantum point contacts, namely, a zero-bias anomaly.[28] This has also been seen in experiments by Ghosh *et al.*[29] Finally, if transport is through metallic domains with discrete states, then one might expect to see an oscillatory thermopower as a function of the gate bias. This has also recently been observed in experiments.[30] Electric field penetration studies of the compressibility could be used to confirm that the system is breaking up into metallic and insulating domains, as has been seen in large area 2D systems.[10]

ACKNOWLEDGMENTS

We thank Arindam Ghosh, Oleg Sushkov, and Erio Tosatti for useful discussions. A.R.H. acknowledges support from an ARC APF grant.

[1] P. W. Anderson, Phys. Rev. **109**, 1492 (1958).
[2] N. F. Mott, Adv. Phys. **16**, 49 (1967).
[3] R. Peierls, Proc. Phys. Soc. London **A49**, 72 (1937).
[4] R. Landauer, J. Appl. Phys. **23**, 779 (1952).
[5] R. W. Keyes, Appl. Phys. **8**, 251 (1975).
[6] R. Landauer, Unpublished note for the National Academy of Sciences Ad Hoc Committee on the Fundamentals of Amorphous Semiconductors, 29 January 1971.
[7] J. Shi and X. C. Xie, Phys. Rev. Lett. **88**, 086401 (2002).
[8] G. Eytan, Y. Yayon, M. Rappaport, H. Shtrikman, and I. Bar-Joseph, Phys. Rev. Lett. **81**, 1666 (1998).
[9] S. Ilani, A. Yacoby, D. Mahalu, and H. Shtrikman, Phys. Rev. Lett. **84**, 3133 (2000).
[10] G. Allison, E. A. Galaktionov, A. K. Savchenko, S. S. Safonov, M. M. Fogler, M. Y. Simmons, and D. A. Ritchie, Phys. Rev. Lett. **96**, 216407 (2006).
[11] S. Das Sarma, M. P. Lilly, E. H. Hwang, L. N. Pfeiffer, K. W. West, and J. L. Reno, Phys. Rev. Lett. **94**, 136401 (2005).
[12] M. J. Manfra, E. H. Hwang, S. Das Sarma, L. N. Pfeiffer, K. W. West, and A. M. Sergent, Phys. Rev. Lett. **99**, 236402 (2007).
[13] L. A. Tracy, E. H. Hwang, K. Eng, G. A. Ten Eyck, E. P. Nordberg, K. Childs, M. S. Carroll, M. P. Lilly, and S. Das Sarma, Phys. Rev. B **79**, 235307 (2009).
[14] A. B. Davydov, B. A. Aronzon, D. A. Bakaushin, and A. S. Vedeneev, Fiz. Tekh. Poluprovodn. **36** 1241 (2002) [Sov. Phys. Semicond. **36**, 1163 (2002)].
[15] S. Adam, S. Cho, M. S. Fuhrer, and S. Das Sarma, Phys. Rev. Lett. **101**, 046404 (2008).
[16] E. Shimshoni, A. Auerbach, and A. Kapitulnik, Phys. Rev. Lett. **80**, 3352 (1998).
[17] Y. Meir, Phys. Rev. B **61**, 16470 (2000).
[18] D. Neilson, J. S. Thakur, and E. Tosatti, Aust. J. Phys. **53**, 531 (2000).
[19] G. Finkelstein, P. I. Glicofridis, R. C. Ashoori, and M. Shayegan, Science **289**, 90 (2000).
[20] S. Chakraborty, I. J. Maasilta, S. H. Tessmer, and M. R. Melloch, Phys. Rev. B **69**, 073308 (2004).
[21] M. Baenninger, A. Ghosh, M. Pepper, H. E. Beere, I. Farrer, and D. A. Ritchie, Phys. Rev. Lett. **100**, 016805 (2008).
[22] N. F. Mott, Philos. Mag. **19**, 835 (1969).
[23] E. Shimshoni and A. Auerbach, Phys. Rev. B **55**, 9817 (1997).
[24] M. Büttiker, IBM J. Res. Dev. **32**, 63 (1988).
[25] V. Tripathi and M. P. Kennett, Phys. Rev. B **74**, 195334 (2006).
[26] D. Popović, A. B. Fowler, and S. Washburn, Phys. Rev. Lett. **67**, 2870 (1991).
[27] C. Siegert, A. Ghosh, M. Pepper, I. Farrer, D. A. Ritchie, D. Anderson, and G. A. C. Jones, Phys. Rev. B **78**, 081302(R) (2008).
[28] S. M. Cronenwett, H. J. Lynch, D. Goldhaber-Gordon, L. P. Kouwenhoven, C. M. Marcus, K. Hirose, N. S. Wingreen, and V. Umansky, Phys. Rev. Lett. **88**, 226805 (2002); D. Goldhaber-Gordon, H. Shtrikman, D. Mahalu, D. Abusch-Magder, U. Meirav, and M. A. Kastner, Nature (London) **391**, 156 (1998).
[29] A. Ghosh, M. H. Wright, C. Siegert, M. Pepper, I. Farrer, C. J. B. Ford, and D. A. Ritchie, Phys. Rev. Lett. **95**, 066603 (2005).
[30] S. Goswami, C. Siegert, M. Baenninger, M. Pepper, I. Farrer, D. A. Ritchie, and A. Ghosh, Phys. Rev. Lett. **103**, 026602 (2009).